BPT-4000 Hall Thruster Extended Power Throttling Range Characterization for NASA Science Missions

IEPC-2009-085

Presented at the 31st International Electric Propulsion Conference,
University of Michigan • Ann Arbor, Michigan • USA
September 20 – 24, 2009

Richard R. Hofer,[1] Dan M. Goebel,[2] John Steven Snyder,[3] and Izabela Sandler[4]
Jet Propulsion Laboratory, California Institute of Technology, Pasadena, CA 91109 USA

Commercial electric propulsion systems are now being considered as a cost effective solution for competitively awarded science missions such as the NASA Discovery and New Frontiers programs. Aerojet's BPT-4000 Hall thruster, which has been identified as a candidate for near-term use on NASA science missions, has recently completed a 6,750 h qualification life test that demonstrated power throttling from 1 to 4.5 kW. To assess the suitability of extending the operating range further, a test campaign designed to assess the performance and plasma properties of the BPT-4000 over an extended throttling range has been implemented. An inverted-pendulum thrust stand is used for performance measurements. In the near-field plume, an emissive probe, cylindrical Langmuir probe, and current density probes are deployed to measure plasma potential, plasma density, electron temperature, and ion current density. In the far-field plume, an RPA, ExB probe, and emissive probe are used to measure the ion energy, ion species' fractions, and plasma potential. The test campaign has demonstrated a 30X power throttling range from 0.15 to 4.5 kW, corresponding to discharge voltages of 125 to 700 V and discharge currents of 1 to 15 A. An eight hour firing demonstrated uninterrupted operation of the thruster at 0.25 kW (150 V, 1.67 A). At this operating condition, the voltage and current were 20% and 67%, respectively, above the minimum power operating condition of 150 V, 1.0 A that the thruster was operated at during the test campaign. The cathode remained healthy throughout testing and was capable of operating without a heater or keeper despite the currents required while at low-power. An initial assessment of the thruster operating at discharge voltages in excess of 400 V has demonstrated the growth potential of this thruster to operate efficiently at specific impulses greater than 2500 s.

Nomenclature

e	=	elementary charge
g	=	acceleration of gravity
I_b, I_d, I_e, I_i	=	current of the ion beam (ΣI_i), the discharge (I_b+I_e), the electrons, and the ith ion species
$I_{sp,a}$	=	anode specific impulse ($T/\dot{m}_a g$)
i	=	ion charge-stage index (1, 2, 3, etc.)

[1] Senior Engineer, Electric Propulsion Group, richard.r.hofer@jpl.nasa.gov.
[2] Senior Research Scientist, Propulsion and Materials Engineering Section.
[3] Senior Engineer, Electric Propulsion Group.
[4] Space Grant Fellow, Electric Propulsion Group.

$\dot{m}_a$, $\dot{m}_b$, $\dot{m}_c$, $\dot{m}_i$, $\dot{m}_t$	=	mass flow rate of the anode, the ion beam ($\Sigma\dot{m}_i$), the cathode, the ith ion species, and the total ($\dot{m}_a + \dot{m}_c$)
m_e, m_{xe}	=	electron and xenon atom mass
N	=	total number of ion species
P_d, P_{jet}, P_{mag} , P_t	=	power of the discharge ($V_d I_d$), the jet (or beam) ($T^2/2\dot{m}_t$), the electromagnet coils, and the total input ($P_d + P_{mag}$)
t	=	time
T	=	thrust
V_a, V_d, V_l	=	acceleration voltage (V_d - V_l), discharge voltage, ion loss voltage
V_p	=	plasma potential
Z_i	=	charge-state of the ith ion species (1, 2, 3, etc.)
Δ	=	Discharge current oscillation amplitude
ε	=	electron current fraction, I_e/I_d
η_a, η_b, η_c, η_d, η_{mag}, η_m, η_q, η_v, η_t	=	anode efficiency, current utilization efficiency, cathode efficiency ($\dot{m}_a/\dot{m}_t$), plume divergence utilization efficiency, electromagnet coil efficiency (P_d/P_t), mass utilization efficiency, charge utilization efficiency, voltage utilization efficiency, total efficiency
θ	=	plume divergence half-angle
τ	=	sampling period
ξ	=	exchange ratio, $m_{xe}I_d/\dot{m}_a e$
Ω_i	=	current fraction of the ith ion species, I_i/I_b

I. Introduction

COMMERCIAL Hall thruster systems are now being considered as a cost effective solution for competitively awarded science missions such as NASA's Discovery and New Frontiers programs [1]. A candidate Hall thruster system is Aerojet's BPT-4000, which has completed a 6,750 h extended life test that demonstrated power throttling from 1 to 4.5 kW [2,3]. The BPT-4000 has been thoroughly characterized over 3.0-4.5 kW, the power range that is used in commercial applications, with more limited measurements below 3.0 kW. In support of a program to qualify the BPT-4000 for NASA science missions, the present study aims to characterize the BPT-4000 operating below 3.0 kW through detailed performance and plume measurements. Specific to these goals, a test campaign was implemented to measure the low power performance, identify operating margins, demonstrate multi-hour firings of the thruster at the sub-kW level, aid in the development of predictive life models through the collection of detailed plasma properties [4,5], and assess the growth potential of the thruster through performance measurements at discharge voltages in excess of 400 V.

On-going experiments are being performed in a large vacuum chamber at the Jet Propulsion Laboratory (JPL). An inverted-pendulum thrust stand is used for performance measurements. Arrays of plasma probes in the near- and far-field are used to measure plume properties. In the near-field (<2 thruster outer diameters), an emissive probe, cylindrical Langmuir probe, and current density probes are deployed to measure plasma potential, plasma density, electron temperature, and ion current density. In the far-field (>5 thruster outer diameters), an RPA, ExB probe, and emissive probe are used to measure the ion energy, ion species' fractions, and plasma potential.

In this paper, initial results from the data set collected during the experiments are described, with an emphasis on operation below 1.0 kW. An overview of the objectives of the test campaign is given in the next section, followed by a description of the experimental apparatus. Results and discussion from the experiments are then presented, which include a detailed look at the performance of the thruster during operation at 0.15 to 1.0 kW, a sampling of plume plasma measurements taken at select operating conditions, and high-voltage (500-700 V) performance measurements. To date, our results indicate that the BPT-4000 is capable of operation over a factor of thirty in discharge power, from 0.15 to 4.5 kW, making it among the most versatile electric propulsion systems currently under consideration for primary propulsion on NASA science missions.

II. Overview of the Experiments

The experiments described here are being performed as part of a larger effort to delta-qualify the BPT-4000 Hall Thruster Propulsion System (HTPS) for near-term use on NASA science missions. Other activities related to this effort include life qualification testing at low-power, efforts to develop predictive lifetime models of the thruster, assessments of the flight readiness of the xenon feed system and power processing unit, and the development of throttle tables that account for the measured variation of performance over thruster life [1-6].

A large volume of data spanning operation from 0.15 to 4.5 kW has been collected to date. However, due to on-going testing and time-constraints analyzing this extensive data set, only a limited portion of the data focusing primarily on operation below 1.0 kW are presented here. Future publications are planned that will present further results.

The primary objectives of the test campaign are as follows:

1. Verify the BPT-4000 throttle tables currently in use at JPL.
2. Demonstrate operating margin over the throttle table in terms of discharge voltage, discharge current, coil current, and cathode flow fraction.
3. Map the performance of the BPT-4000 over the full operating envelope currently possible within the limits of the flight-qualified Power Processing Unit (PPU) and thruster.
4. Identify the minimum discharge voltage, current, and power where reliable operation of the thruster is possible.
5. Collect plasma property data in the near-field plume of the thruster and cathode and far-field plume necessary for validating outputs of computational performance and lifetime models.
6. Demonstrate multi-hour operation of the thruster at low power (<1 kW).

Secondary objectives of this test campaign that are being pursued as resources allow:

1. Measure the performance of the thruster at discharge voltages greater than 400 V, up to a maximum of 800 V and discharge power of 4.5 kW.
2. Repeat a limited portion of the performance and plume measurements listed above with discharge chamber insulator rings corresponding to the erosion geometry observed after the end of Aerojet's qualification life testing.

III. Experimental Apparatus

A. BPT-4000 Hall Thruster

The BPT-4000 HTPS was developed through a joint effort between Lockheed Martin Space Systems and Aerojet as a 4.5 kW electric propulsion system for GEO satellite applications [2,7]. The first flight of the BPT-4000 is scheduled for 2010. The qualification life test (QLT) for GEO applications of this system was completed in 2005 [7,8], and was subsequently extended through a NASA funded qualification life test extension (QLT-E) during which extended operation at low-power (1-2 kW) was demonstrated. Aerojet has also measured sub-kW performance and plume properties down to discharge powers of 0.3 kW [2]. Measurements presented here have demonstrated operation as low as 0.15 kW. Table 1 summarizes the total impulse, operating time, thruster starts, and propellant throughput that were demonstrated through the end of the QLT-E. Erosion measurements indicated that very little erosion was observed during the QLT-E. Aerojet erosion models of the BPT-4000 predict that a total of 11.3 MN-s and 580 kg of xenon throughput are possible before the magnetic circuit is exposed to the high-energy plasma [6]. The qualified life and throttling capabilities of the BPT-4000 and its low-cost relative to government systems make it a very attractive candidate for near-term infusion in cost-capped science missions such as the NASA Discovery and New Frontiers programs.

Table 1. Demonstrated and predicted capability of the BPT-4000 Hall thruster [2,3,6].

Parameter	BPT-4000 Demonstrated [2,3]	BPT-4000 Predicted [6]
Total Impulse	5.3 MN-s	11.3 MN-s
Total Firing Time	6,750 h	14,400 h
Total Thruster Starts	6,844	>6,844
Total Xenon Throughput	272 kg	580 kg

Experiments were performed with an Engineering Model (EM) BPT-4000 thruster and cathode [9]. A photograph of the thruster installed on the thrust stand in the vacuum chamber is shown in Figure 1. The boron nitride insulator rings of the discharge chamber were pre-machined to the geometry resulting after 1,200 h of thruster operation during the Aerojet qualification life test [2,3]. This condition is used because the thruster performance closely matches the average performance over the full life test at this point in the thruster's life. The insulators were conditioned by operating the thruster for over 25 h before acquiring performance and plume data.

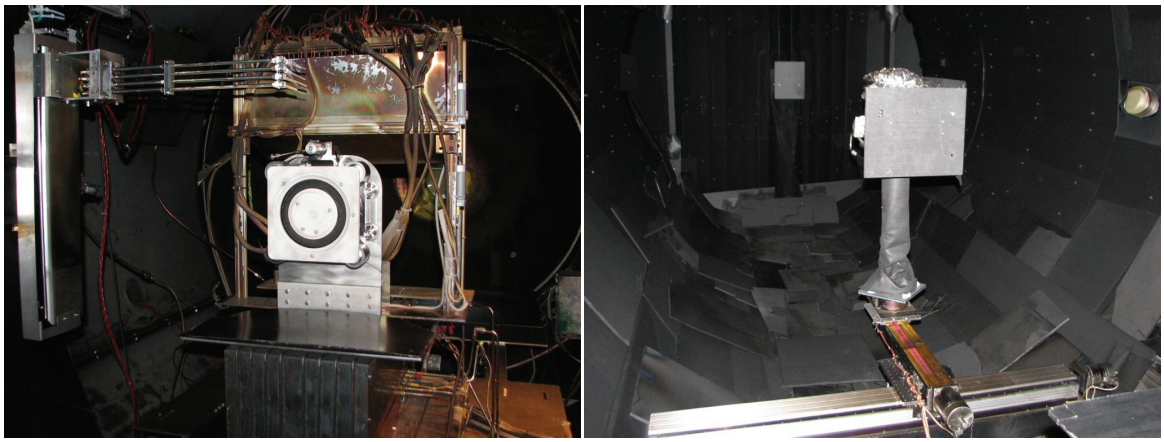

Figure 1. Photographs of the experimental configuration showing the thruster installed on the thrust stand and the near-field probe array (left) and the far-field probe array (right).

B. Vacuum Facility

Experiments were performed in the Endurance Test Facility (ETF) at JPL. The 3 m diameter by 10 m long vacuum chamber has been used previously to test Hall thrusters at power levels up to 10 kW [4,10,11]. The facility is cryogenically pumped and is lined with graphite panels to minimize backsputtered material to thruster surfaces. Base pressures between 10^{-8} and 10^{-7} torr are routinely achieved. At the maximum xenon flow rate of 15.43 mg/s, the operating pressure in the ETF was 1.3×10^{-5} torr, equivalent to a pumping speed of 170 kl/s.

C. Power Electronics and Propellant Delivery System

Power and propellant were delivered to the BPT-4000 with commercially available power supplies and flow controllers. The plasma discharge was sustained by a pair of power supplies wired in series capable of 1000 V, 20 A operation. The discharge filter consisted of a 80 μF capacitor in parallel with the discharge power supply outputs. Additional power supplies were used to power the magnet coils and the cathode heater and keeper. The cathode heater and keeper were used only during the thruster ignition sequence. Research-grade xenon (99.9995% pure) was supplied through stainless steel feed lines with 50 and 500 sccm mass flow controllers. The controllers were calibrated before the experiment and were digitally controlled with an accuracy of ±1% of the set point.

D. Thrust Stand

Thrust measurements were acquired using a water-cooled, inverted-pendulum thrust stand with inclination control and active damping. Upon initial exposure to vacuum, the thruster was operated for at least two hours to allow for outgassing of thruster components. Thrust measurements were typically conducted at constant power, in intervals of 30 to 60 minutes, following the outgassing procedure. Thermal drift and inclination were accounted for during post-processing.

It is generally accepted in the Hall thruster community that pressures of less than 2×10^{-5} Torr are sufficient to reliably obtain performance measurements without needing to correct for neutral gas ingestion [12,13]. This criterion was met in these experiments and no attempts to correct for neutral ingestion were made.

Calibrations were performed daily by deploying a series of known weights ten times each. As shown in Figure 2, these weights spanned the range of 39 to 302 mN. When inclination and thermal drift were accounted for, the response of the thrust stand was repeatable and linear to the applied force. Thrust levels as low as 10 mN were measured in these experiments, which were less than the calibrated thrust range. Owing to the highly linear response of the thrust stand and repeatability of the measurements, uncertainty due to being outside of the calibrated thrust range was judged to be negligible. Thermal drifts of the thrust stand zero are typically the single largest uncertainty in the measurement. These drifts are partially offset at low-power due to the much reduced thermal

loads on the thrust stand. Initial analysis of thrust stand uncertainty indicated a range of ±1-2%, with the largest uncertainty occurring at the lowest power. Given the uncertainty of the thrust, mass flow rate, current, and voltage, the propagated uncertainty for specific impulse was estimated as ±1.4-2.8% and ±2.3-4.6% for efficiency, again with the largest uncertainty occurring at the lowest power.

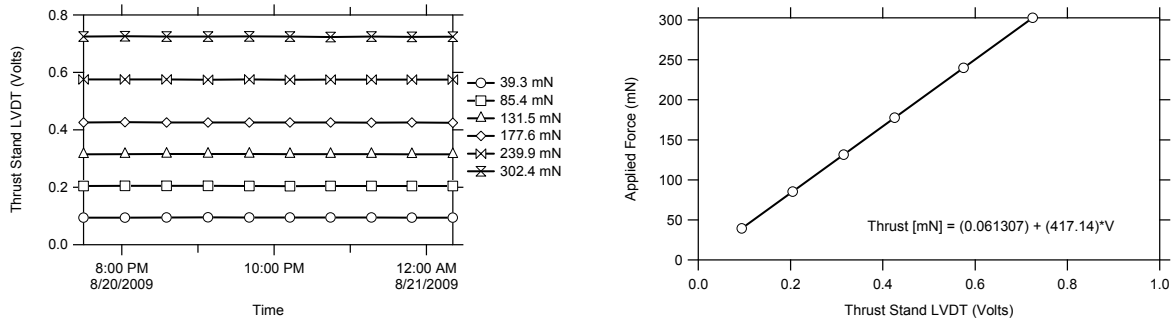

Figure 2. Thrust stand calibration results. Left: LVDT response to calibration weights. Right: Thrust stand calibration curve.

E. Discharge Current Probe

A pair of 20 MHz current probes and an 8-bit, 500 MHz oscilloscope were used to measure discharge current oscillations during steady-state thruster operation with an accuracy of ±3%. The current probes were located on the anode and cathode sides of the power input between the thruster and capacitor described above. The probes were physically located outside the vacuum chamber, near the feedthrough used to feed power in to the chamber. Oscillations were quantified by calculating the oscillation amplitude of the discharge current defined by

$$\Delta \equiv \frac{1}{\langle I_d \rangle} \sqrt{\frac{\int_0^\tau \left[I_d(t) - \langle I_d \rangle \right]^2 dt}{\tau}}, \tag{1}$$

where $I_d(t)$ is the time-dependent discharge current, $\langle I_d \rangle$ is the time-averaged discharge current, and τ is the sampling period.

F. Near-field Plasma Probes

Near-field plume plasma parameters are being investigated using an array of scanning probes using methodologies similar to those described in Ref. [11,14]. To date, measurements of the plasma properties have been taken at the 4.5 kW (300 V, 15 A) power level. Additional measurements at lower discharge power are on-going. The near-field scanning probe drive system and the probe array are shown in the test chamber with the BPT-4000 in Figure 1. Figure 3 is a close-up photograph of the near-field probe array. The probe diagnostics consisted of a cylindrical Langmuir probe to measure the local electron temperature, a flat disk probe oriented perpendicular to the thruster axis to measure the ion current density in the beam, an emissive probe to measure the local plasma potential, and a cylindrical probe configured to measure only the radial ion current density.

Measurements of the plasma parameters were made by scanning the array radially across the thruster face with the probe tips located at a series of positions axially from the thruster exit plane. This provides radial profiles of the plasma parameters at different axial distances from 0.36 cm to 30 cm downstream of the thruster exit plane. When the probe array was not in use, it was parked out of the plume in the farthest upstream axial position, about 7 cm above the cathode axis.

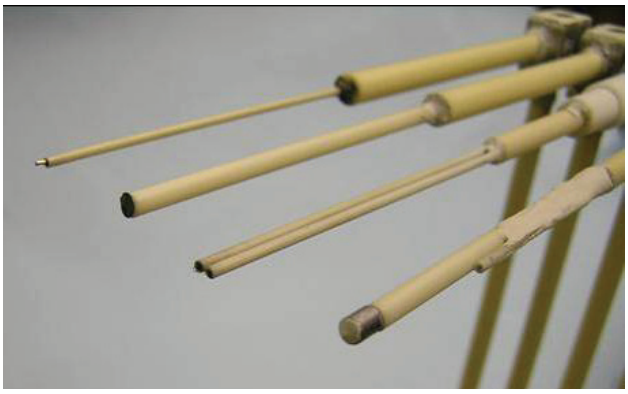

Figure 3. Photograph of the near-field probe array showing (from left to right) the cylindrical Langmuir probe for measurements of the electron temperature and plasma potential, flat disk probe for measurements of the axial ion current density, emissive probe for measurements of the plasma potential, and a cylindrical probe configured only to measure the radial ion current density.

G. Far-field Plasma Probes

Shown in the right photograph of Figure 1, an array of plasma probes were deployed in the far-field plume region. The probe array consisted of an ExB probe, a Retarding Potential Analyzer (RPA), and an emissive probe, that were used to measure ion species fractions, ion energy, and plasma potential, respectively. The probes were positioned in the plume using a pair of linear translation stages and a rotary stage. The axial position was varied depending on the thruster discharge power. For discharge power less than 1.0 kW, the probes were 1.07 m downstream of the thruster exit plane and for discharge power greater than 1.0 kW, the probes were 1.5 m downstream of the thruster. The radial position of the probes was aligned with the mid-channel radius of the thruster, with the probes rotated to align with the local current density vector, which roughly resulted in the probes being pointed at the center of the thruster. The direction of the current density vector was determined by measuring the probe current as a function of angle. For the ExB probe, the probe was biased to the voltage corresponding to the Xe^+ ion species and for the RPA the probe was biased to the voltage corresponding to the maximum in the ion voltage distribution.

1. ExB Probe

An ExB probe, or Wien filter, is a band-pass ion filter that selects ions according to their velocities through the application of crossed electric and magnetic fields [15,16]. Because the velocity of multiply-charged ions in Hall thrusters is proportional to the square root of their charge-state, an ExB probe can be used to discriminate between ion species. Analysis of the ion current from the probe characteristic can then be used to compute the ion species fractions.

The ExB probe used in these experiments was used previously with other high-power Hall thrusters [10,16]. Following Shastry's method to maintain plume attenuation due to charge-exchange collision less than 30% [16], the probe was positioned downstream of the thruster such that the maximum product of the pressure and distance was $p*z = 2x10^{-5}$ Torr-m. Analysis of the probe spectra and a correction accounting for the loss of main beam ions due to charge-exchange collisions also followed Shastry's method [16].

Measurements of the ion species fractions were accomplished using the single sampling location described above. Although a more accurate measurement would account for the azimuthal distribution of multiply-charged ions in the plume through multiple measurements weighted by the local current density, Reid found that results accurate to within 1.5% of the plume-weighted average could be obtained through a single measurement when the probe was radially located on the mid-channel radius and pointed at the thruster center [17]. Based on Reid's results, a single sampling location was used as this choice balances well the accuracy of the measurement and the time required to obtain it.

The combined standard uncertainty of the ion species fractions computed from the ExB probe spectra has been estimated as 3% in Xe^+, and 20% in Xe^{2+} and Xe^{3+}.

2. Retarding Potential Analyzer (RPA)

A retarding potential analyzer (RPA) selectively filters ions by applying a retarding potential across an inlet grid [18]. The probe acts as a high-pass filter by allowing only ions with voltages (i.e., energy-to-charge ratios) greater

than the grid voltage to pass and reach a collection electrode. The derivative of the resulting current-voltage characteristic is then proportional to the ion voltage distribution function.

The RPA used in this investigation was a modified version of the probe described in [18]. The modified probe includes a pair of ion retarding grids to improve the uniformity of the electric field used to filter the ions and improve the energy resolution of the probe. Measurements of the ion voltage distribution were taken with respect to facility ground. Plasma potential (V_p) measurements taken with the emissive probe, which was identical in construction to the probe described in Ref. [11], were used to correct the RPA data so that the true ion voltage distribution could be computed, i.e., $V_{true} = V_{rpa} - V_p$. The most-probable ion voltage (V_{mp}) and the ion loss voltage (V_l) were then found from the true ion voltage distribution. The most-probable ion voltage was defined as the voltage where the ion current was greatest. The ion loss voltage was then computed as the difference between the discharge voltage and the most-probable ion voltage, i.e., $V_l = V_d - V_{mp}$. The uncertainty of the most-probable voltage was estimated as ±1%.

IV. Results and Discussion

Objectives 1-4 in section II relate to characterizing the performance and operating margins of the BPT-4000 over its operational envelope. Throttle tables in use at JPL serve as the starting point for these investigations. Figure 4 shows the current-voltage combinations of the JPL throttle tables. Excursions in discharge voltage, discharge current, cathode flow rate, and magnet coil current beyond those specified in the throttle tables have been conducted to demonstrate operating margin and gain additional performance data for this thruster.

Figure 5 shows the current-voltage combinations that were considered during the performance mapping. Various limits are implicit to these operating conditions, which are driven by considerations of the limits of the thruster and/or PPU. The maximum discharge power was limited to 4.5 kW, as this was the design limit for the thruster. The current PPU limits the maximum current to 15 A and the voltage range to 150-400 V in 50 V increments. The regions identified in Figure 5 are:

I. V_d = 150-400 V, I_d = 2-15 A. This region maps the operating envelope within the limits of what has been previously demonstrated or known to be a limit due to the existing hardware limits. The most detailed performance maps were generated in this region.

II. V_d = 125-150 V, I_d = 2-15 A. This region was considered to demonstrate voltage margin below the 150 V minimum voltage of the current PPU design.

III. V_d = 125-400 V, I_d = 1-2 A. This region was considered during efforts to identify the minimum operating current where stable, reliable operation and performance of the thruster was realized.

IV. V_d = 400-800 V, I_d = 1-11.25 A. This region is currently beyond the capability of the PPU and is being considered to characterize the high-voltage performance of the thruster.

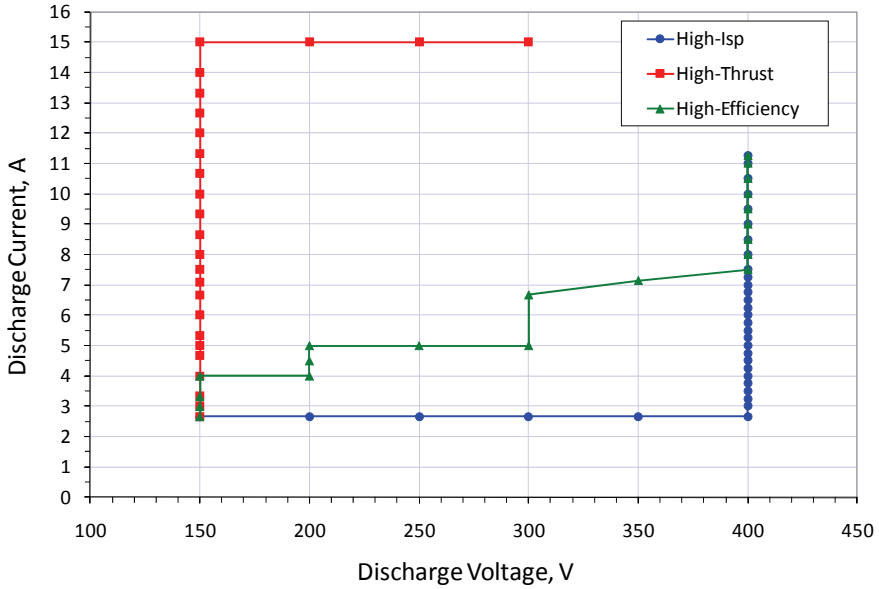

Figure 4. Current-voltage combinations for various BPT-4000 throttle tables in use at JPL.

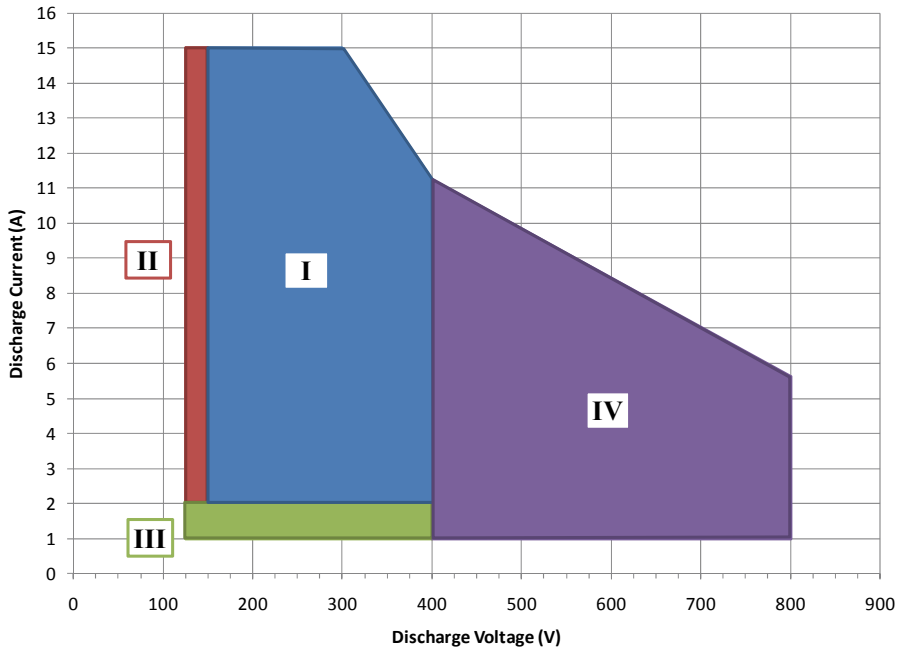

Figure 5. Current-voltage combinations for BPT-4000 performance testing.

For a given discharge voltage and current, consideration was given to the effects of the following on performance:

1. **Magnet coil current** – For operating conditions that are well characterized (1-4.5 kW), coil currents from qualification testing at Aerojet were generally used. Outside of this range, performance maps as a function of coil current were generated with the aim of identifying maximum efficiency.
2. **Cathode flow fraction** – The flight flow system specifies the cathode flow fraction as 5-9% of the anode flow rate as the nominal range. Excursions over this range were considered at a limited number of operating conditions to characterize the sensitivity of the thruster to these variations. Additionally, below total flow rates of 9 mg/s, the flight flow system is incapable of maintaining the nominal flow split, resulting in cathode flow fractions greater than 9%. Excursions from the nominal, to higher flow fractions, were conducted for these cases in order to determine the sensitivity of the cathode and thruster to the cathode flow rate.
3. **Keeper and/or heater power** – Nominal operation of the flight system does not power the keeper or heater during steady-state operation. Testing found that operation of the keeper or heater was unnecessary over the full range of operation that was demonstrated (0.15 to 4.5 kW).

A. Reference Firing (3.0-4.5 kW, 300-400 V)

For commercial applications, the BPT-4000 is operated at four conditions corresponding to 3.0 or 4.5 kW discharge power and 300 or 400 V discharge voltage. These are the most well characterized operating conditions for the thruster and serve as a reference point for verifying nominal operation of the thruster and the test facility. Performance at these operating conditions is shown in Table 2, which are consistent with the published performance of the thruster [7,9]. Specific impulse and efficiency include cathode flow rate, but, to be consistent with Aerojet convention, efficiency is shown excluding thermally-dependent magnet and cabling losses. At maximum operating temperatures, these losses are typically 1.5% of the total power.

The JPL experiments are conducted using insulator rings pre-machined to the erosion geometry after 1,200 h of thruster operation. This point was chosen because at this point performance is very close to the time-averaged value [2,7]. Figure 6 and Table 3 compare the measured thrust over 6,750 h of BPT-4000 operation, the time-averaged thrust, and the thrust measured at JPL with insulator rings pre-machined to the 1,200 h erosion geometry. Measurements at JPL deviate from the time-averaged thrust by only 0.4-1.8%, indicating that JPL measurements are representative of the time-averaged performance of the BPT-4000.

Table 2. Performance measured at JPL of the BPT-4000 at the operating conditions used for commercial applications.

Operating Condition	Thrust (mN)	Total Specific Impulse (s)	Efficiency* (-)
4.5 kW, 300 V	279	1843	0.56
4.5 kW, 400 V	251	2019	0.55
3.0 kW, 300 V	193	1744	0.55
3.0 kW, 400 V	172	1917	0.54

* Excludes thermally-dependent magnet and cabling losses. At maximum operating temperatures, these losses are typically 1.5% of the total power.

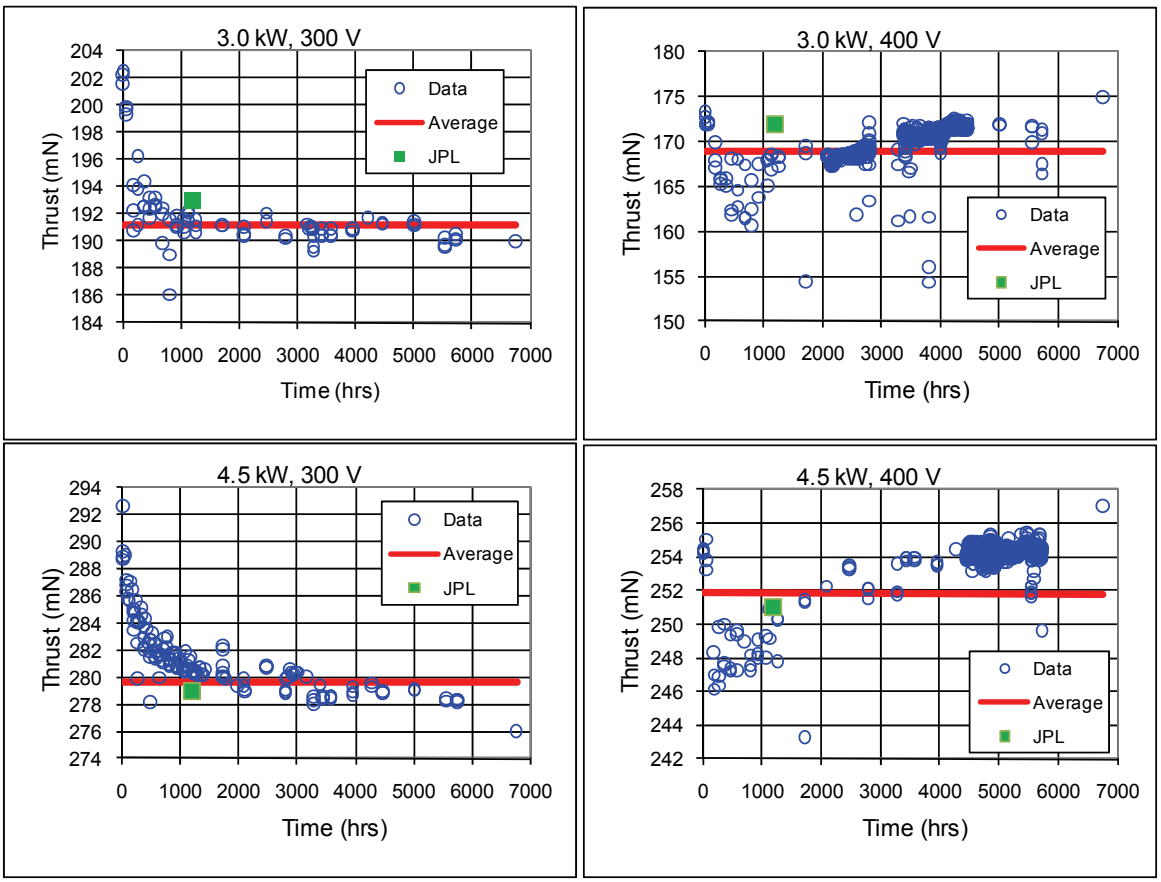

Figure 6. Comparison of the measured thrust over 6,750 h of BPT-4000 operation, the time-averaged thrust, and the thrust measured at JPL with insulator rings pre-machined to the 1,200 h erosion geometry. Measurements at JPL deviate from the time-averaged thrust by only 0.4-1.8%, indicating that JPL measurements are representative of the time-averaged performance of the BPT-4000.

Table 3. Comparison of the time-averaged thrust measured during qualification testing at Aerojet and thrust measured at JPL using the 1,200 h insulator rings. Measurements at JPL deviate from the time-averaged thrust by only 0.4-1.8%, indicating that JPL measurements are representative of the time-averaged performance of the BPT-4000.

Operating Condition	Thrust - QLT Avg. (mN)	Thrust - JPL (mN)	% Difference
4.5 kW, 300 V	280	279	0.4%
4.5 kW, 400 V	252	251	0.4%
3.0 kW, 300 V	191	193	-1.0%
3.0 kW, 400 V	169	172	-1.8%

B. Power Throttling

The discharge current-voltage combinations that have thus far been investigated are shown in Figure 7. Current throttling over 1-15 A and voltage throttling from 125-700 V have been demonstrated. The lowest power was 0.15 kW (150 V, 1A), which is equivalent to a 30X power throttling from the maximum power of 4.5 kW. Operation at 0.15 kW was sustained for over an hour on two separate testing days before being voluntarily terminated on both occasions. All conditions investigated were stable, repeatable, and within thermal margins. The thruster was operated for at least 20 minutes at each operating condition, including those operating conditions demonstrated primarily to demonstrate operating margin (e.g., discharge voltage of 125 V or discharge currents of 1.0 A). Overall, the results indicate that the BPT-4000 is a continuously variable thruster over at least 0.15-4.5 kW, 125-700 V.

A photograph of the thruster operating at 0.15 kW is shown in Figure 8. Despite a 15X throttling ratio in current, visual observations of the discharge chamber displayed a high-degree of azimuthal uniformity. All other operating conditions were also found to have a high-degree of azimuthal uniformity.

Figure 9 shows the coupling voltage for all operating conditions tested during the experiments. Typical values were -11 to -14 V for this cathode. The cathode used during the Aerojet qualification life test historically ranged from -10.5 to -13.5 V, which is indicated in Figure 9 as the shaded region for reference. At the lowest power of 0.15 kW (1 A), the cathode potential was -14.3 V. We found that the cathode potential exceeded -15 V for only a few operating conditions when the current was less than 2 A. Throughout testing, the cathode ignition voltage remained between 15 to 25 V and showed no dependence on the operating condition. Cathode potentials always returned to nominal values when the thruster was returned to 4.5 kW operation after several hours of testing below 1.0 kW. Overall, there were no indications that cathode health was negatively impacted by low-power operation.

Keeper voltage oscillations were measured for a limited number of operating conditions, primarily at low-power. Powering either the keeper or the heater was found to be unnecessary during any of the operating conditions investigated here. Measurements were taken with the keeper unpowered and floating. The magnitude of the cathode keeper voltage oscillations (typically expressed as peak-to-peak values), is commonly used in the ion thruster literature to judge whether the cathode is operating in spot or plume mode. This transition is important in ion thrusters, as it has been found to correlate with enhanced keeper erosion [19]. Values of 5 V peak-to-peak are typically adopted to mark this transition. Besides being an arbitrary value, it is not clear whether this metric is relevant to the health of the cathode during Hall thruster operation. Since these measurements were taken with the keeper electrode unpowered and floating, coupling of the keeper electrode to the discharge current oscillations could not be ruled out. We found the peak-to-peak keeper voltage oscillations to be 8.9 V throughout the multi-hour demonstration at 150 V, 1.67 A described below. However, measurements taken during qualification life testing at Aerojet ranged from 10 to 25 V for discharge currents ranging from 5 to 15 A. Given that the thruster operated for 6,750 h and exhibited virtually no measurable erosion of the keeper or cathode orifice, it seems that keeper voltage oscillations are not a relevant metric in Hall thruster operation.

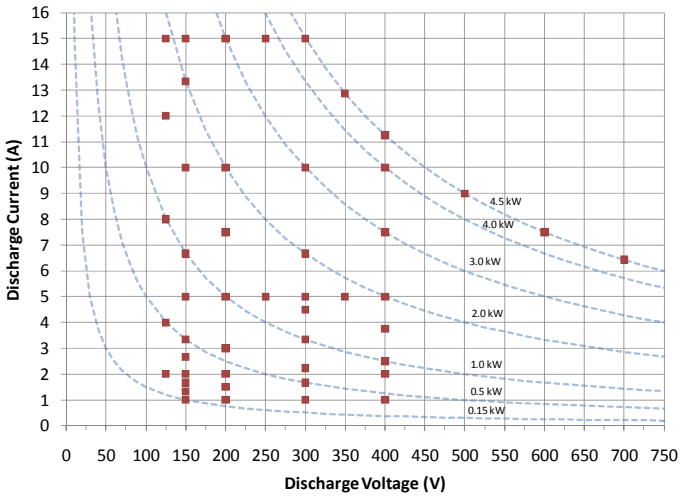

Figure 7. Operating conditions investigated during performance investigations. Lines of constant discharge power are drawn for reference. The BPT-4000 demonstrated current throttling from 1-15 A and voltage throttling from 125-700 V.

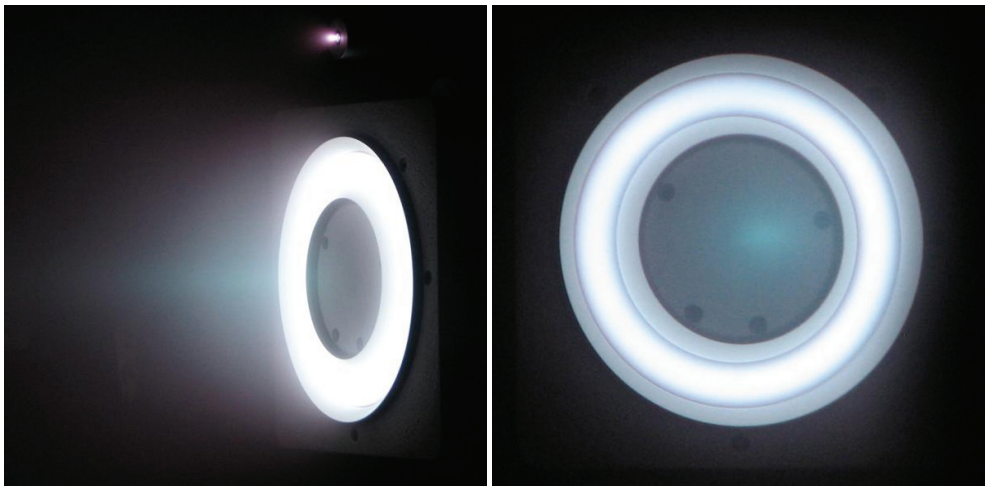

Figure 8. Photographs of the BPT-4000 operating at 0.15 kW, 1.0 A. Despite being operated 30X below the maximum power and 15X below the maximum current, the discharge displayed a very high degree of azimuthal uniformity.

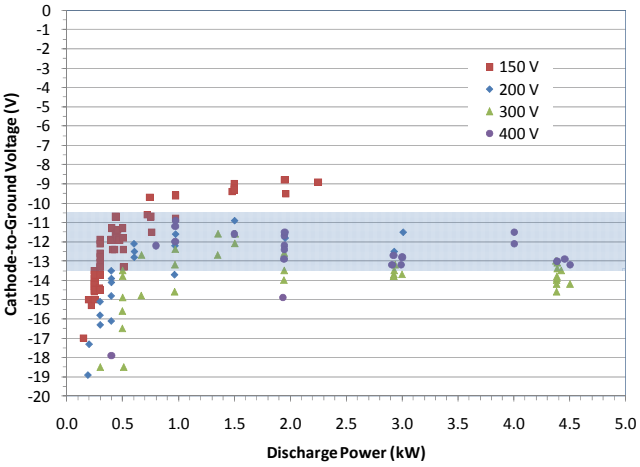

Figure 9. Cathode coupling voltage versus discharge power. The shaded region indicates the historical range observed during qualification life testing at Aerojet.

C. Low-Power Performance

In this section, we focus our discussion on the performance of the BPT-4000 operating at discharge powers less than 1.0 kW. Additional data spanning 1.0-4.5 kW is under analysis and will be presented in future publications.

The flow split in the flight flow controller for GEO applications is greater than 9% for total flow rates less than 9 mg/s. For deep space applications, we anticipate modifying the propellant flow system by adding an additional orifice and a pair of latch valves, controlled by the spacecraft bus, so that the flow fraction can be maintained to within 10-20% of the anode flow rate. The flow split will purposely be maintained at a high level for low power operation in order to maintain a minimum level of flow rate to the cathode of about 0.24 mg/s (i.e., equivalent to the minimum flow rate for the discharge cathode in the NSTAR ion thruster).

The effects of cathode flow rate on performance were assessed for several operating conditions. Figure 10 presents the results from one such study during operation at 150 V, 2 A. A nearly proportional decrease in specific impulse and efficiency results for flow fractions of 10-20%. Cathode coupling voltage over the same range varied from -13.3 V to -11.9 V. In general, it was found that the cathode coupling voltage would remain above -14 V for a wide range of cathode flow splits and that flow splits of 10-15% were a good balance between maintaining cathode coupling voltage and thruster efficiency.

The cathode heater and keeper were used only during thruster startup for all conditions investigated. An investigation of the effects of keeper current on thruster performance was undertaken at 150 V, 2 A. Figure 11 shows the effects of keeper current on the cathode voltage and thruster efficiency for keeper currents ranging from 0 to 1 A. Coupling voltage and efficiency are unchanged up to 0.2 A and then begin to have a negative impact on these parameters. Other than these parameters, thruster operation was unchanged. Additional studies at other operating conditions yielded similar results.

Based on test results to date, performance, plume, and long-duration testing performed at JPL and Aerojet has revealed no indications that operation at the reduced flow rates necessary for low-power operation have been detrimental to cathode or thruster health [2,3]. Coupling voltages are within nominal ranges. Over firing times of several hours, the coupling voltage is constant. The cathode keeper and heater were not required to maintain steady operation. Ignition voltages also remained nominal during multiple thruster restarts at low power and the cathode coupling voltages returned to nominal values when the thruster was operated later at high power. Additional efforts are underway to assess further the operating environment of the cathode under low power operation. These efforts include near-field plume measurements, internal plasma and temperature measurements, and plasma modeling.

Figure 12 through Figure 14 present thrust, specific impulse, and efficiency for discharge voltages of 150-400 V and discharge power ranging from 0.15 to 1.00 kW. Specific impulse and efficiency include cathode flow and magnet power. The cathode keeper and heater were not used. Thrust ranged from a minimum of 10 mN to a maximum of 76 mN. Specific impulse ranged from 490 (still better than a chemical rocket!) to 1450 s. Efficiency ranged from 15 to 45%.

Putting aside considerations involving the cathode already discussed above, determining the optimum means to throttle the thruster down in power must also consider the minimum current and voltage (including a margin allowance) for reliable operation and the effects of the operating conditions on the performance, plume divergence, and lifetime. Assessments related to plume divergence and lifetime will be conducted in the near-term, but we do not anticipate any major risk items. These investigations have shown that the thruster can be operated at any combination of 125-400 V and 1-15 A. The performance data here suggests that at the lowest power operating conditions that operating at 200 V or greater and 1.5 A or greater will maximize performance. This is shown in Figure 14 where we see that 200 V operation results in higher efficiency when the thruster is operated above 0.2 kW. A throttle table that maximizes efficiency based on these results is shown in Table 4.

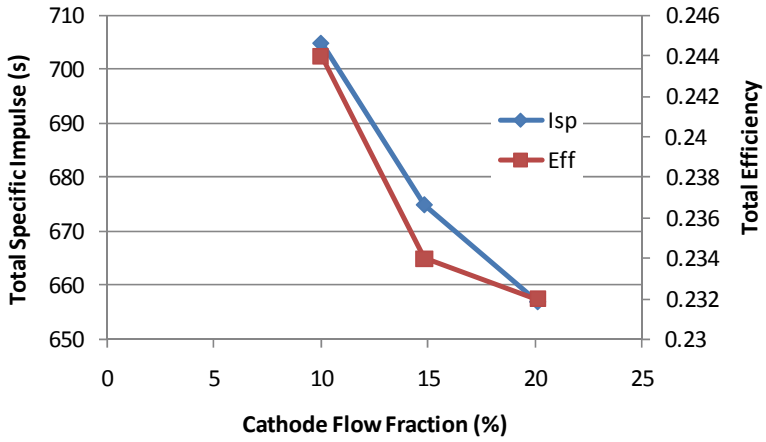

Figure 10. Total specific impulse and total efficiency versus cathode flow fraction during operation at 150 V, 2 A.

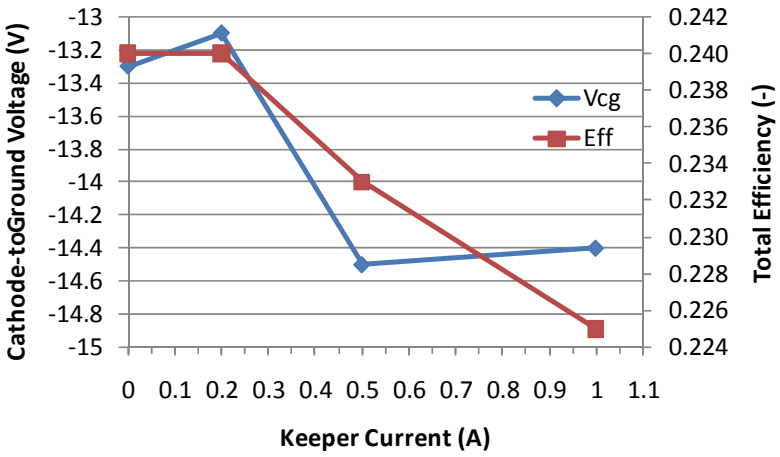

Figure 11. Cathode coupling voltage and total efficiency versus keeper current during operation at 150 V, 2 A.

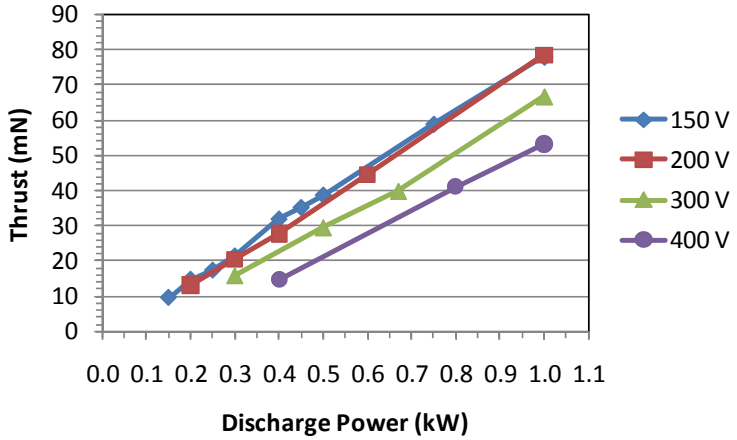

Figure 12. Thrust versus discharge power.

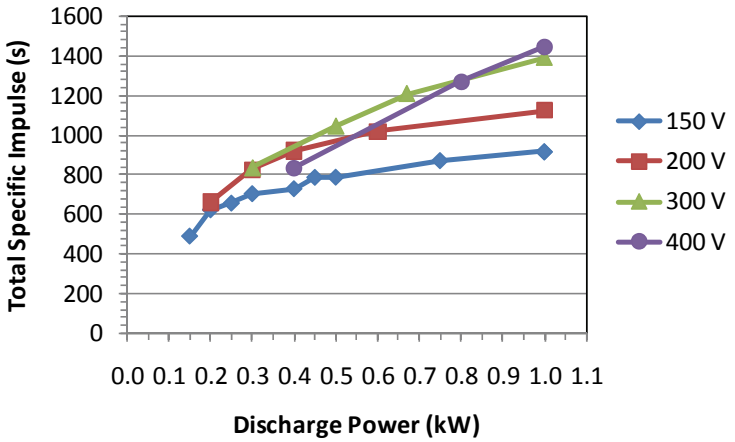

Figure 13. Total specific impulse versus discharge power.

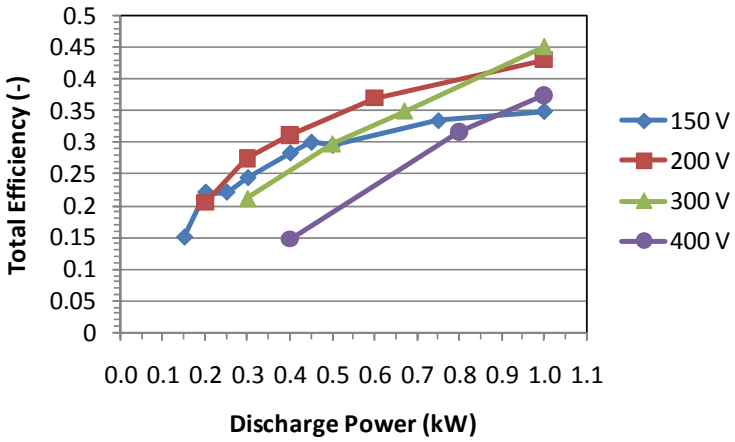

Figure 14. Total efficiency versus discharge power.

Table 4. Low-power throttle table maximizing efficiency below 0.40 kW.

Pd (kW)	Vd (V)	Id (A)
0.225	150	1.50
0.250	150	1.67
0.300	200	1.50
0.400	200	2.00

D. Multi-hour, Low-power Demonstration

An important objective of the test campaign was the planned multi-hour firing of the thruster at a selected low-power operating condition. Operation at 0.25 kW (150 V, 1.67 A) was selected although all data indicated that any of the operating conditions down to 0.15 kW could have been chosen with similar results. At this operating condition, the voltage and current were 20% and 67%, respectively, above the minimum power operating condition of 150 V, 1.0 A that the thruster was operated at during the test campaign. Results from an eight hour firing of the thruster at 0.25 kW are shown in Figure 15. Thrust measurements are not available because the thermal drift of the thrust stand could not be accounted for during this extended firing. The thruster was started from a "cold" condition after being left off overnight in the vacuum chamber. The discharge was started at 150 V, 1.5 A initially, and then after one hour, the current was increased to 1.67 A. Anode flow rate was adjusted during the demonstration in order to maintain 1.67 A of discharge current. After approximately four hours, the flow rate did not require further

adjustment and the discharge current reached a steady-state. After eight hours had elapsed, the thruster was voluntarily turned off. The cathode coupling voltage with respect to ground experienced minor excursions over the range of -14 to -15.5 V for the first three hours, but then remained within a few tenths of a volt of -14.5 V thereafter. The coil voltage, which is usually taken as an indication of the bulk temperature of the thruster, only began to reach steady-state at the conclusion of the demonstration. This was not unexpected due to the low power of the discharge. Ignition voltages and coupling voltage for the cathode were all nominal during the next day of testing. The magnitude of discharge current oscillations was constant over the course of testing. Overall, the multi-hour test demonstrated that the BPT-4000 is capable of reliable, stable operation at 0.25 kW.

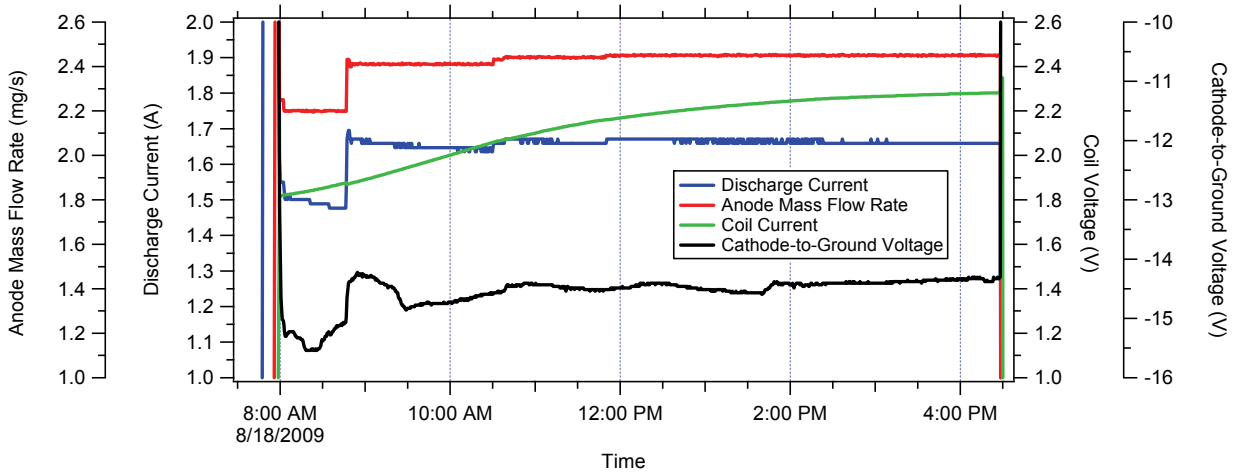

Figure 15. Thruster telemetry during the multi-hour firing of the BPT-4000 at 0.25 kW (150 V, 1.67 A).

E. Near-field Probe Data

Results from the near-field probes analyzed to date include measurements of the plasma potential, electron temperature, and ion current density at 300 V, 15 A.

Electron temperature measurements were taken during the radial scans of the near-field probe array with the 0.5 mm diameter, 2 mm long cylindrical Langmuir probe shown in Figure 3. The left plot in Figure 16 shows an example of the classical Langmuir characteristic plotted on a semi-log plot of data taken on the thruster axis and 3 cm downstream of the exit plane. The fit to the exponential region shows an electron temperature at this location of 4.3 eV. The well-defined break in the knee of the trace gives a local plasma potential of 32 eV, which is in good agreement with emissive probe data to be discussed later. An example of the Langmuir probe characteristics obtained in the channel region is shown in the right plot in Figure 16, which was taken 0.4 cm downstream of the thruster exit. The local electron temperature from the exponential fit is about 14 eV. In this location, the emissive probe showed the plasma potential to be much higher than that found on the thruster axis, but the Langmuir probe voltage was not swept sufficiently positive to determine the potential.

Plasma potential profiles were obtained from radial scans of the emissive probe shown in Figure 3. The emissive probe consisted of a short loop of 0.127 mm diameter tungsten wire that was spot welded to 0.5 mm diameter tantalum connection wires fed through two 1 mm diameter ceramic tubes. The 10 cm long tantalum wires were then hard-soldered to 1 mm diameter copper wire fed to a floating heater supply to minimize the voltage drop in the connections. The emissive probe was operated in the hot-floating-potential mode where the filament is heated to emissive temperatures and the probe then floats near the local plasma potential. Figure 17 shows examples of the radial variation of plasma potential at axial locations of 3 cm and 10 cm from the thruster exit plane from the emissive probe data. Close to the thruster exit the cathode plume could be seen as the most negative potential, but this potential depression disperses rapidly moving away from the cathode and the thruster exit plane.

Axial profiles of the plasma potential relative to the cathode potential and the electron temperature, on the center of the channel and the thruster axis, were constructed from the radial probe scans and are shown in Figure 18. Plasma potential data that was taken with the cylindrical Langmuir probe and the emissive probe on the channel center is also shown for comparison. The data are in reasonable agreement, and certainly within the uncertainty of each technique. The plasma potential in the channel near the thruster exit plane was found to be about 70 V, and decreased to about 34 V 30 cm downstream of the exit. The electron temperature from the Langmuir probe data shows that the temperature approaches 15 eV near the thruster exit plane, and decreases rapidly to about 4.2 eV 30

cm from the thruster. On the axis of the thruster, the potential peaks several centimeters downstream of the exit plane and then decreases to about 34 V at 30 cm from the thruster. The electron temperature on axis is also about 4.2 eV at all locations downstream beyond about 3 cm from the thruster. The radial scans show that the electron temperature is very uniform in the plume beyond about 5 cm downstream of the thruster exit plane.

The ion flux in the thruster plume was measured by two of the probes shown in Figure 3. The flat disk probe was about 3 mm in diameter, and was constructed with 3 mm diameter ceramic tubing touching the back surface to shield collection except from the front. The radial probe was also 3 mm in diameter and shielded both front and back such that only ion flux on the sides were collected. Both probes were biased at -45 V relative to ground to collect ion saturation current. Figure 19 shows the ion current density collected by the two probes during a radial scan 0.36 cm downstream of the thruster exit plane. Interestingly, the collected ion flux was nearly the same directly in front of the cathode as in the channel region. Also, the radial flux was an order of magnitude less than the axial flux in the cathode and channel region, but was comparable to the axial flux near the thruster centerline and between the cathode and the channel.

Further downstream in the plume, the ion current density measured by the probes shows that the cathode plume disperses rapidly and the channels coalesce to form a more uniform beam. The left plot in Figure 20 shows the radial ion current density profiles from the two probes at a distance of 2.5 cm from the thruster exit plane. The ion flux at the cathode radius has decreased more than an order of magnitude, even though the channel current density is essentially unchanged. Far out in the plume the channel peaks coalesce to form a uniform beam, as seen in the right plot in Figure 20 taken 30 cm from the thruster exit plane.

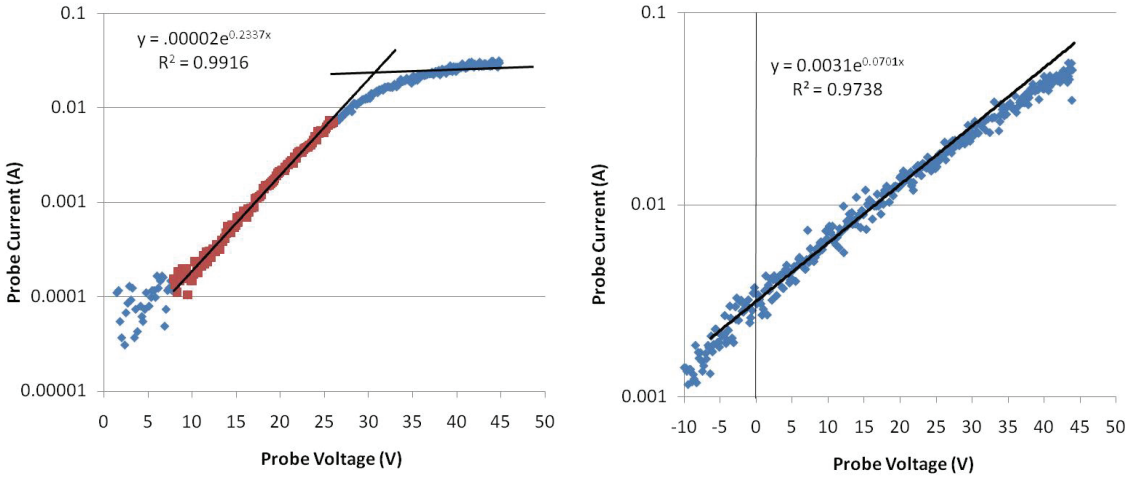

Figure 16. Examples of Langmuir probe traces obtained on the thruster axis 3 cm from the thruster exit (left), and in the center of the channel 0.4 cm downstream of the thruster exit (right) during thruster operation at 300 V, 15 A.

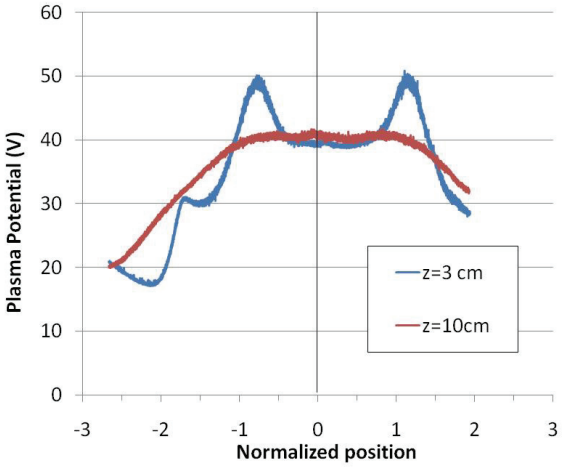

Figure 17. Radial variation of the plasma potential from the emissive probe for scans at 3 cm and 10 cm from the thruster exit during thruster operation at 300 V, 15 A. Position is normalized to the mid-channel radius of the thruster.

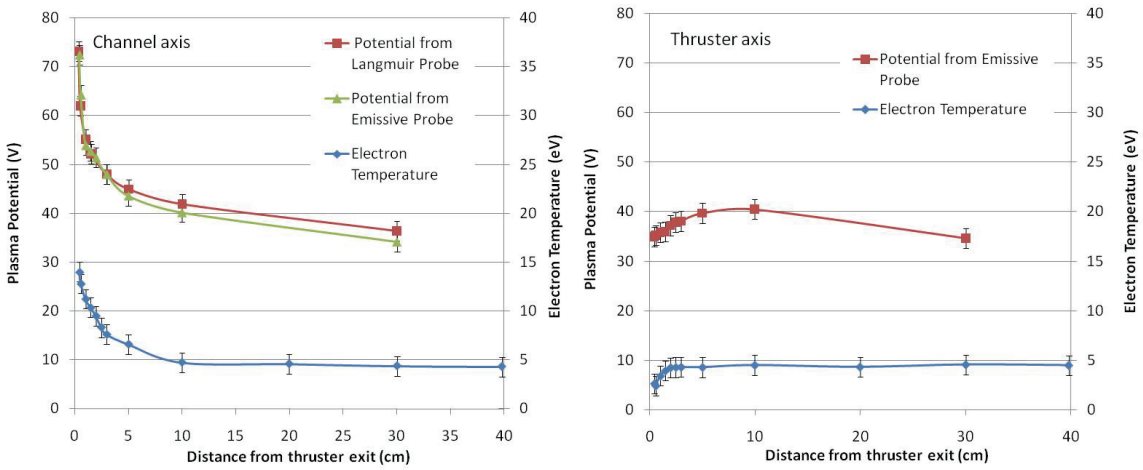

Figure 18. Axial plasma potential profile and electron temperature from the thruster exit measured at the center of the channel (left) and at the center of the thruster (right) during thruster operation at 300 V, 15 A. Plasma potential is relative to the cathode potential.

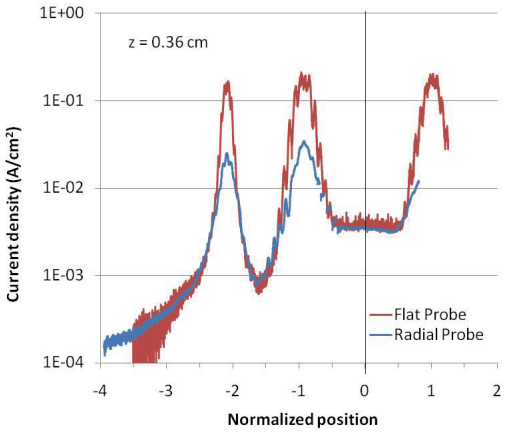

Figure 19. Current density measurements from the flat probe and the radial probe at a distance of 0.36 cm from the thruster exit during thruster operation at 300 V, 15 A. Position is normalized to the mid-channel radius of the thruster, with the origin located at the thruster centerline.

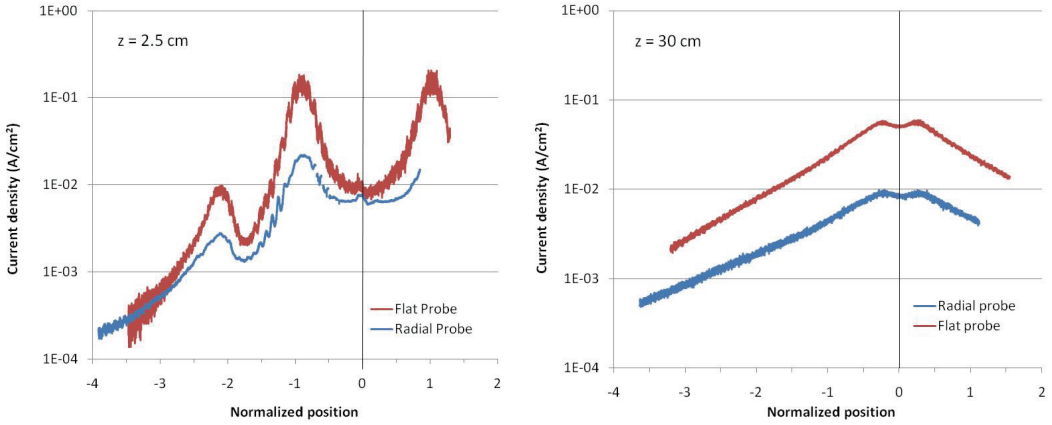

Figure 20. Current density measurements from the flat probe and the radial probe at a distance of 2.5 cm (left) and 30 cm (right) from the thruster exit during thruster operation at 300 V, 15 A. Position is normalized to the mid-channel radius of the thruster, with the origin located at the thruster centerline.

F. Far-Field Probe Data

Results from the far-field probes analyzed to date include measurements of the ion species fractions, plasma potential, and ion energy at 300 V, 15 A and 150 V, 1.67 A. Figure 21 presents far-field probe results during operation at 150 V, 1.67 A as measured by the RPA (left) and the ExB probe (right). The low discharge current contributed to a noticeable dearth of elastic broadening in the RPA scan typically seen at higher currents. The low discharge voltage also eliminated any detection of triply-charged xenon in the ExB scan. Table 5 summarizes the results for operation at 300 V, 15 A and 150 V, 1.67 A and also includes calculations of the utilization efficiencies as defined in Ref. [4] and partially repeated as follows.

Excluding the electrical efficiency of the systems that deliver power to a Hall thruster, the total thrust efficiency (η_t) is the ratio of jet power in the exhaust to the total input power

$$\eta_t = \frac{P_{jet}}{P_t} = \frac{T^2}{2\dot{m}_a P_d}\frac{P_d}{P_t}\frac{\dot{m}_a}{\dot{m}_t} = \eta_a \eta_{mag} \eta_c \,. \tag{2}$$

The cathode efficiency (η_c) and electromagnet efficiency (η_{mag}) account for the cathode flow rate and the power supplied to the electromagnet coils, respectively. The anode efficiency is the thrust efficiency neglecting power to the magnets or the cathode flow rate and is the product of the five utilization efficiencies given by

$$\eta_a = \frac{T^2}{2\dot{m}_a P_d} = \eta_q \eta_v \eta_d \eta_b \eta_m \,, \tag{3}$$

where the utilization efficiencies for charge, voltage, plume divergence, current, and mass are given by

$$\eta_q = \frac{\left(\sum \Omega_i / \sqrt{Z_i}\right)^2}{\sum \Omega_i / Z_i},\ \eta_v = \frac{V_a}{V_d} = 1 - \frac{V_l}{V_d},\ \eta_d = \left(\cos\theta\right)^2,\ \eta_b = \frac{I_b}{I_d} = 1 - \varepsilon,\ \eta_m = \frac{\dot{m}_b}{\dot{m}_a} = \xi \eta_b \sum \frac{\Omega_i}{Z_i}. \tag{4}$$

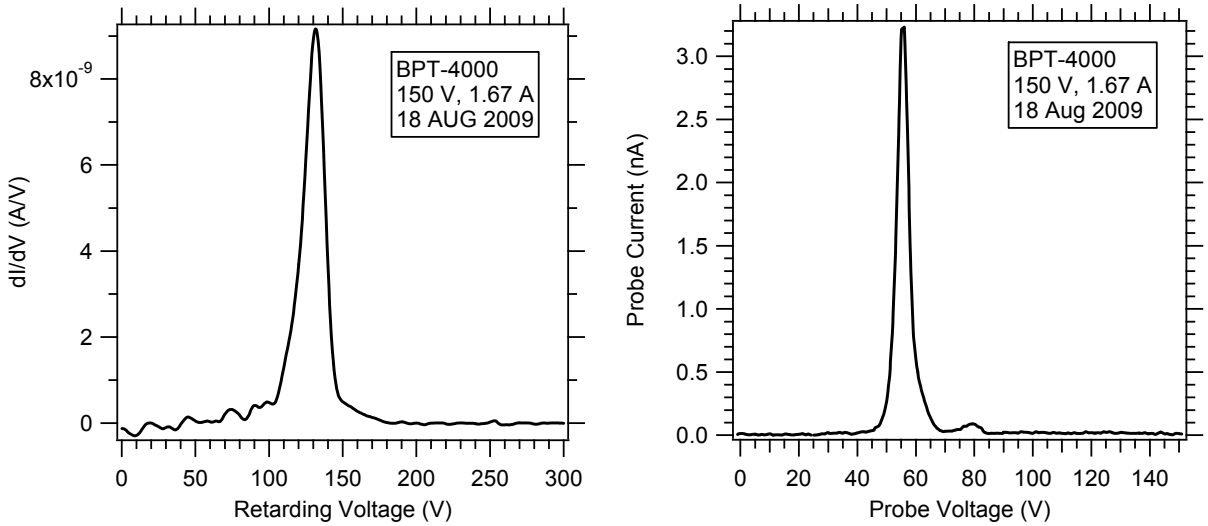

Figure 21. Far-field probe results during 150 V, 1.67 A operation as measured by the RPA (left) and the ExB probe (right). The low discharge current contributed to a noticeable dearth of elastic broadening in the RPA scan typically seen at higher currents. The low discharge voltage also eliminated any detection of triply-charged xenon in the ExB scan

Table 5 includes a value of 11.84 A for the ion current. This result was computed by integrating the ion current density profile shown in Figure 19 over the channel width and is equivalent to a beam current utilization of 0.789. The voltage and charge utilizations were 0.902 and 0.979, respectively, while the mass utilization was 0.983. The

mass utilization was high for a Hall thruster, with values of 0.90-0.95 being more typical. The divergence utilization was 0.874, equivalent to a 20.8 degree divergence angle. Overall, the high-efficiency of the BPT-4000 at 300 V, 15 A is largely attributed to the high mass utilization.

The power spectra of the discharge current oscillations measured on the anode side of the plasma are presented in Figure 22 for operation at 300 V, 15 A and 150 V, 1.67 A. The breathing-mode is more diffuse at the high-power condition than at the low-power one. Table 6 summarizes various characteristics of the discharge current oscillations. Peak-to-peak current oscillations were measured to be 14.24 A at 300 V, 15 A, consistent with measurements taken during qualification life testing at Aerojet. The breathing-mode frequency reduces from 19-22 kHz at the high-power condition to 4.7 kHz at the low-power condition. This reduction is expected due to the lower discharge voltage, since the breathing-mode scales to first order as the square root of the ion velocity.

Table 5. Various measured properties of the BPT-4000 and calculated values from a performance model during operation at 300 V, 15 A and 150 V, 1.67 A.

	300 V, 15 A	150 V, 1.67 A
Measured Values		
Ion energy (V)	271	125
Loss voltage (V)	29	25
Xe+ current fraction	0.772	0.952
Xe2+ current fraction	0.184	0.048
Xe3+ current fraction	0.043	0
Beam current (A)	11.84	-
Thrust (mN)	278.6	17.4
Anode Isp (s)	1972	724
Anode Efficiency (-)	0.599	0.247
Calculated Values		
Exchange Ratio	1.417	0.929
Voltage Utilization	0.902	0.835
Charge Utilization	0.979	0.996
Current Utilization	0.789	-
Mass Utilization	0.983	-
Divergence Utilization	0.874	-
Divergence Half-Angle (deg)	20.8	-

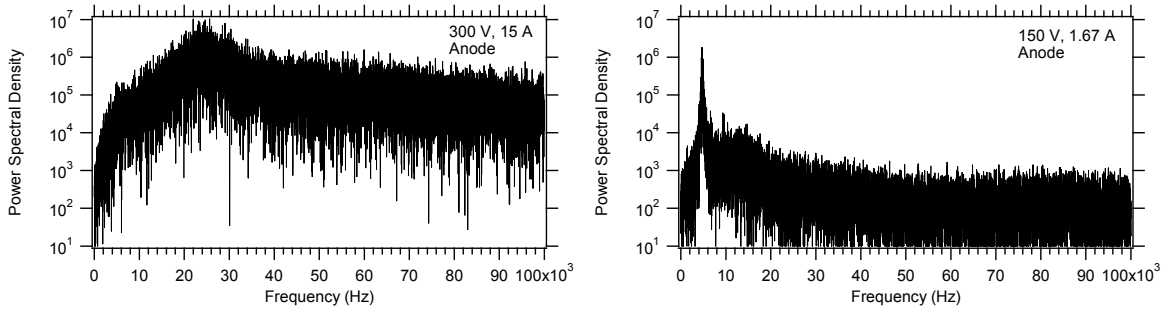

Figure 22. Discharge current power spectral density measured at the anode versus frequency for operation at 300 V, 15 A (left) and 150 V, 1.67 A (right).

Table 6. Characteristics of the discharge current oscillations for operation at 300 V, 15 A and 150 V, 1.67 A.

	300 V, 15 A	150 V, 1.67 A
	Anode	
Osc. Amp. (A) =	1.09	0.11
P2P (A) =	14.24	0.90
f (kHz) =	22	4.7
	Cathode	
Osc. Amp. (A) =	0.68	0.12
P2P (A) =	8.24	0.89
f (kHz) =	19.4	4.7

G. High-Voltage Performance

As presently designed, the BPT-4000 propulsion system is capable of maximum discharge voltages of 400 V, corresponding to about 2000 s specific impulse. Near-term implementation of the BPT-4000 would be limited by these specific impulses, but missions further afield would benefit if a higher specific impulse range could be attained. Such a change would require changes to the output voltage of the PPU discharge supply. Upgrades to the voltage isolation, coil design, and changes to the life rating may also be required. In order to assess the potential growth of the BPT-4000 system to higher specific impulses, preliminary performance measurements at discharge voltages of 500-700 V and 4.5 kW were taken. Figure 23 shows the total specific impulse and total efficiency of the thruster operating over 300-700 V, 4.5 kW. Cathode flow rate and coil power are included in the figure. Efficiency is a nearly constant 55% over this voltage range, with a minor decrease to 53% observed at 700 V. Specific impulse ranged from 2220-2570 s over 500-700 V. Performance improvements may be possible with further optimization of the magnetic coils. Additional measurements are planned to further characterize the thruster at high-voltage, but these initial results indicate that the BPT-4000 operates efficiently at specific impulses in excess of 2500 s.

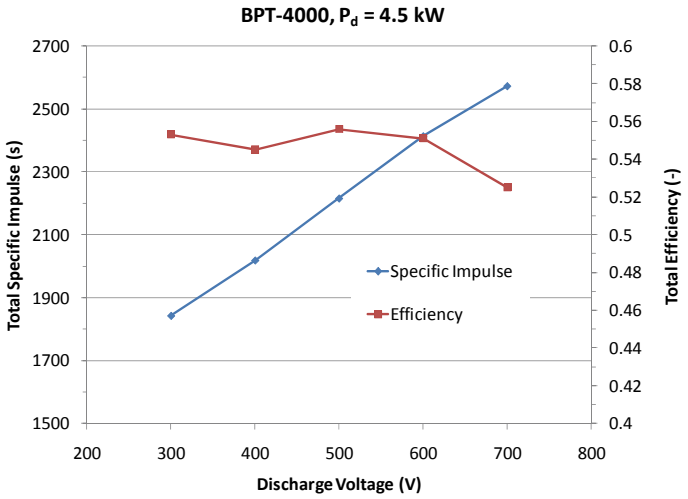

Figure 23. Total specific impulse and total efficiency versus discharge voltage at a constant discharge power of 4.5 kW.

V. Conclusion

A test campaign designed to assess the performance and plasma properties of the BPT-4000 has demonstrated a 30X power throttling range from 0.15 to 4.5 kW, corresponding to discharge voltages of 125 to 700 V and discharge currents of 1 to 15 A. An eight hour firing demonstrated uninterrupted operation of the thruster at 0.25 kW (150 V, 1.67 A). At this operating condition, the voltage and current were 20% and 67%, respectively, above the minimum power operating condition of 150 V, 1.0 A that the thruster was operated at during the test campaign. The cathode remained healthy throughout testing and was capable of operating without a heater or keeper despite the currents required while at low-power. To date, performance, plume, and long-duration testing performed at JPL and Aerojet has revealed no indications that operation at the reduced flow rates necessary for low-power operation have been detrimental to cathode or thruster health [2,3]. An initial assessment of the thruster operating in excess of 400 V has

demonstrated the growth potential of this thruster to achieve specific impulses greater than 2500 s. Additional testing and analysis of the thruster at low-power and high-voltage are on-going and will be reported in future publications.

Acknowledgments

The research described in this paper was carried out at the Jet Propulsion Laboratory, California Institute of Technology, under a contract with the National Aeronautics and Space Administration.

These experiments would not have been possible without the generous loan of the BPT-4000 that was provided by Aerojet and Lockheed Martin. We would like to thank Kristi DeGrys at Aerojet and Vadim Khayms at Lockheed Martin for supporting the hardware loan and Alex Mathers at Aerojet for preparing the thruster and providing excellent support for the experiments throughout.

References

[1] Hofer, R. R., Randolph, T. M., Oh, D. Y., Snyder, J. S., and De Grys, K. H., "Evaluation of a 4.5 kW Commercial Hall Thruster System for NASA Science Missions," AIAA Paper 2006-4469, July 2006.

[2] De Grys, K. H., Carpenter, C., Welander, B., Mathers, A., Hofer, R. R. et al., "Extended Duration Operation of BPT-4000 Qualification Unit at Low Power," Presented at the 3rd JANNAF Spacecraft Propulsion Joint Subcommittee Meeting, Orlando, FL, Dec. 8-12, 2008.

[3] Hofer, R. R., Mikellides, I. G., Katz, I., and Goebel, D. M., "BPT-4000 Hall Thruster Discharge Chamber Erosion Model Comparison with Qualification Life Test Data," Presented at the 30th International Electric Propulsion Conference, IEPC Paper 2007-267, Florence, Italy, Sept. 17-20, 2007.

[4] Hofer, R. R., Katz, I., Mikellides, I. G., Goebel, D. M., Jameson, K. K. et al., "Efficacy of Electron Mobility Models in Hybrid-PIC Hall Thruster Simulations," AIAA Paper 2008-4924, July 2008.

[5] Mikellides, I. G., Katz, I., Hofer, R. R., and Goebel, D. M., "Hall-Effect Thruster Simulations with 2-D Electron Transport and Hydrodynamic Ions," Presented at the 31st International Electric Propulsion Conference, IEPC-2009-114, Ann Arbor, MI, Sept. 20-24, 2009.

[6] Randolph, T. M., "Qualification of Commercial Electric Propulsion Systems for Deep Space Missions," Presented at the 30th International Electric Propulsion Conference, IEPC Paper 2007-271, Florence, Italy, Sept. 17-20, 2007.

[7] De Grys, K. H., Welander, B., Dimicco, J., Wenzel, S., Kay, B. et al., "4.5 kW Hall Thruster System Qualification Status," AIAA Paper 2005-3682, July 2005.

[8] Welander, B. A. and De Grys, K. H., "Completion of the BPT-4000 Hall Thruster Qualification," Presented at the 53rd JANNAF Propulsion Meeting, Monterey, CA, Dec. 5-8, 2005.

[9] Mathers, A., De Grys, K. H., and Paisley, J., "Performance Variation in BPT-4000 Hall Thrusters," Presented at the 31st International Electric Propulsion Conference, IEPC-2009-144, Ann Arbor, MI, Sept. 20-24, 2009.

[10] Hofer, R. R., Johnson, L. K., Goebel, D. M., and Wirz, R. E., "Effects of Internally-Mounted Cathodes on Hall Thruster Plume Properties," IEEE Transactions on Plasma Science 36, 5, 2004-2014 (2008).

[11] Jameson, K. K., Goebel, D. M., Hofer, R. R., and Watkins, R. M., "Cathode Coupling in Hall Thrusters," Presented at the 30th International Electric Propulsion Conference, IEPC Paper 2007-278, Florence, Italy, Sept. 17-20, 2007.

[12] Hofer, R. R. and Gallimore, A. D., "High-Specific Impulse Hall Thrusters, Part 1: Influence of Current Density and Magnetic Field," Journal of Propulsion and Power 22, 4, 721-731 (2006).

[13] Biagioni, L., Kim, V., Nicolini, D., Semenkin, A. V., and Wallace, N. C., "Basic Issues in Electric Propulsion Testing and the Need for International Standards," Presented at the 28th International Electric Propulsion Conference, IEPC Paper 2003-230, Toulouse, France, March 17-21, 2003.

[14] Jameson, K. K., "Investigation of Hollow Cathode Effects on Total Thruster Efficiency in a 6 kW Hall Thruster," Ph.D. Dissertation, Aerospace Engineering, University of California, Los Angeles, 2008.

[15] Hofer, R. R. and Gallimore, A. D., "Ion Species Fractions in the Far-Field Plume of a High-Specific Impulse Hall Thruster," AIAA Paper 2003-5001, July 2003.

[16] Shastry, R., Hofer, R. R., Reid, B. M., and Gallimore, A. D., "Method for Analyzing Exb Probe Spectra from Hall Thruster Plumes," Review of Scientific Instruments 80, 063502 (2009).

[17] Reid, B. M., Shastry, R., Gallimore, A. D., and Hofer, R. R., "Angularly-Resolved Exb Probe Spectra in the Plume of a 6-kW Hall Thruster," AIAA Paper 2008-5287, July 2008.

[18] Hofer, R. R., Haas, J. M., and Gallimore, A. D., "Ion Voltage Diagnostics in the Far-Field Plume of a High-Specific Impulse Hall Thruster," AIAA Paper 2003-4556, July 2003.

[19] Goebel, D. M., Jameson, K. K., Katz, I., and Mikellides, I. G., "Potential Fluctuations and Energetic Ion Production in Hollow Cathode Discharges," Physics of Plasmas 14, 103508 (2007).